Modeling coronal magnetic field using spherical geometry: cases with several active regions

Tilaye Tadesse[1,2] • T. Wiegelmann[3] • K. Olson[1] • P. J. MacNeice[4]

Abstract The magnetic fields in the solar atmosphere structure the plasma, store free magnetic energy and produce a wide variety of active solar phenomena, like flare and coronal mass ejections(CMEs). The distribution and strength of magnetic fields are routinely measured in the solar surface(photosphere). Therefore, there is considerable interest in accurately modeling the 3D structure of the coronal magnetic field using photospheric vector magnetograms. Knowledge of the 3D structure of magnetic field lines also help us to interpret other coronal observations, e.g., EUV images of the radiating coronal plasma. Nonlinear force-free field (NLFFF) models are thought to be viable tools for those task. Usually those models use Cartesian geometry. However, the spherical nature of the solar surface cannot be neglected when the field of view is large. In this work, we model the coronal magnetic field above multiple active regions using NLFFF extrapolation code using vector magnetograph data from the Synoptic Optical Long-term Investigations of the Sun survey (SOLIS)/ Vector Spectromagnetograph (VSM) as a boundary conditions. We compare projections of the resulting magnetic field lines solutions with their respective coronal EUV-images from the Atmospheric Imaging Assembly (SDO/AIA) observed on October 11, 2011 and November 13, 2012. This study has found that the NLFFF model in spherical geometry reconstructs the magnetic configurations for several active regions which agrees with observations. During October 11, 2011 observation, there are substantial number of trans-equatorial loops carrying electric current.

Keywords Active Regions, Magnetic Fields; Active Regions, Models; Magnetic fields, Corona; Magnetic fields, Photosphere; Magnetic fields, Models

Tilaye Tadesse

Department of Physics, Drexel University, Philadelphia, PA 19104-2875, U.S.A.

[2]Addis Ababa University, College of Natural Sciences, Institute of Geophysics, Space Science, and Astronomy, Po.Box 1176, Addis Ababa, Ethiopia

T. Wiegelmann

Max Planck Institut für Sonnensystemforschung, Max-Planck Str. 2, D–37191 Katlenburg-Lindau, Germany

K. Olson

Department of Physics, Drexel University, Philadelphia, PA 19104-2875, U.S.A.

P. J. MacNeice

NASA, Goddard Space Flight Center, Code 674, Greenbelt, MD 20771, U.S.A.

1 Introduction

The geometry and dynamics of the solar corona are determined by the evolving magnetic field at the Suns surface (photosphere). Thus, magnetic fields are believed to play a dominant role for active phenomena carried out in the solar corona. In order to study solar eruptive phenomena, we have to understand how magnetic energy is stored in the pre-eruptive corona. Hence, the three dimensional (3D) structure of magnetic fields and electric currents in the pre-eruptive corona and the amount of free energy stored in the field have to determined (Schrijver and Title 2005; Jiang and Feng 2012). Unfortunately, reliable magnetic field measurements are still restricted to the level of the photosphere, where the inverse Zeeman effect in Fraunhofer lines is observable. Even if the measurement of magnetic fields in the solar corona has considerably improved in recent decades (Lin et al. 2000; Liu and Lin 2008), further developments are needed before accurate data are routinely available.

As an alternative to measurements in the solar atmosphere, magnetic field extrapolation have been implemented to calculate the field from the measured photo-

spheric field using assumptions that the fields are force-free. In this model assumption, the corona magnetic forces are dominant that all non-magnetic forces like plasma pressure gradient and gravity can be neglected in the lowest order (Gary 2001). This implies that, if there are currents, they must be aligned with the magnetic field. To describe the equilibrium structure of the static coronal magnetic field, the force-free assumption is appropriate:

$$(\nabla \times \mathbf{B}) = \alpha \mathbf{B} \tag{1}$$

$$\nabla \cdot \mathbf{B} = 0 \tag{2}$$

subject to the boundary condition

$$\mathbf{B} = \mathbf{B}_{\rm obs} \quad \text{on photosphere} \tag{3}$$

where $\mathbf{B}$ is the magnetic field and $\mathbf{B}_{\rm obs}$ is measured vector field on the photosphere. Equation (1) states that the currents are co-aligned with magnetic fields, where α is the torsion function that represents the proportionality between the electric current density and the magnetic field. Equation (2) describes the absence of magnetic monopoles.

Parameter α of Equation (1) can be a function of position, but the combination of Equation (1) and Equation (2) ($\mathbf{B} \cdot \nabla \alpha = 0$) requires that α be constant along a given field line. $\alpha = 0$ yields the current-free potential field. If α is constant everywhere in the volume under consideration, the field is called linear force-free field (LFFF), otherwise it is nonlinear force-free field (NLFFF) (Wiegelmann 2004; Wheatland and Régnier 2009; Wheatland and Leka 2011; Wiegelmann et al. 2012; Wiegelmann and Sakurai 2012; Malanushenko et al. 2012). Potential and linear force-free fields can be used as a first step to model the general structure of magnetic fields in the solar corona, the use of nonlinear force free fields is essential to understand eruptive phenomena. Practically there are both observational and theoretical reasons which suggest that the pre-eruptive magnetic fields are non-linear force-free fields. For details of those models we direct the readers to Wiegelmann and Sakurai (2012).

Most of the NLFFF modeling codes are implemented in the Cartesian geometry. Therefore those codes are not well suited for larger domains, since the spherical nature of the solar surface cannot be neglected when the field of view is large. DeResa et al. (2009) has studied that different NLFFF models have different field line configurations in the coronal volume with widely varying estimates of the magnetic free energy. The study suggested that the main reasons for that problem are (1) non-force free nature of the field within the photosphere, (2) the uncertainties on vector-field measurements, particularly on the transverse component, and (3) the needs of large domain that can capture the connections of an active region to its surroundings to accommodate more electric currents associated with the full active regions of interest. Solar Dynamics Observatory (SDO) mission has made repeated observations of large, almost global scale events in which large scale connection between active regions may play fundamental role. Therefore, this needs motivate us to implement a NLFFF procedure in spherical geometry to large scale boundary data from the Helioseismic and Magnetic Imager (HMI) on board SDO and Synoptic Optical Long-term Investigations of the Sun survey (SOLIS)/ Vector Spectromagnetograph (VSM) (Wiegelmann 2007; Tadesse et al. 2009, 2011, 2012a,b; Guo et al. 2012; Tadesse et al. 2013)

Coronal magnetic fields manifest themselves in X-rays and EUV images in the shapes of coronal loops. Those loops provide an additional constraint which is not currently being used due to the mathematical complications of incorporating such input into numerical models (Malanushenko et al. 2012). The 3D structure of magnetic loops from NLFFF models help us for modeling of plasma loops, and understanding coronal heating and plasma flows along the loops. In this work, we apply our spherical NLFFF procedure to a group of active regions observed on October 11, 2011 and November 13, 2012 using SOLIS/VSM data. During the former observation, there were six active regions (ARs 11610, 11611, 11612, 11613, 11614 and 11615) and there were three vertically aligned active regions in later one. In our previous work Tadesse et al. (2012b), we have studied the connectivity between three neighboring active regions which were horizontally aligned. Here, we compare the extrapolated magnetic loops with their respective extreme ultraviolet (EUV) observations by the Atmospheric Imaging Assembly (AIA) on board SDO.

2 Method

This study requires extrapolating the three-dimensional NLFFF coronal fields from the photospheric boundary data. The photospheric vector magnetograms, obtained by the Synoptic Optical Long-term Investigations of the Sun survey (SOLIS)/ Vector Spectromagnetograph (VSM) are used as the boundary conditions. Meanwhile, those measured data are inconsistent with the above force-free assumption. Therefore, one has to apply some transformations to these data before nonlinear force-free extrapolation codes can be applied. This

procedure is known as preprocessing. This preprocessing scheme removes forces and torques from the boundary and approximates the photospheric magnetic field to the low plasma-β force-free chromosphere. For detailed descriptions of the method we direct the readers to Wiegelmann et al. (2006) for Cartesian geometry and Tadesse et al. (2009) for spherical one.

We solve the force-free equations (1)(with the form $\nabla \times \mathbf{B}) \times \mathbf{B} = 0$) and (2) using optimization principle (Wheatland et al. 2000; Wiegelmann 2004) in spherical geometry (Wiegelmann 2007; Tadesse et al. 2009, 2013, 2012c). The method minimizes a joint measure (L_ω) of the normalized Lorentz forces and the divergence of the field throughout the volume of interest, V. Optimization procedure is spherical geometry is given by:

$$L_\omega = L_f + L_d + \nu L_{photo} \tag{4}$$

$$L_f = \int_V \omega_f(r,\theta,\phi) B^{-2} \left|(\nabla \times \mathbf{B}) \times \mathbf{B}\right|^2 r^2 \sin\theta dr d\theta d\phi$$

$$L_d = \int_V \omega_d(r,\theta,\phi) \left|\nabla \cdot \mathbf{B}\right|^2 r^2 \sin\theta dr d\theta d\phi$$

$$L_{photo} = \int_S \mathbf{B}_d \cdot \mathbf{W}(\theta,\phi) \cdot \mathbf{B}_d \, r^2 \sin\theta d\theta d\phi$$

where $\mathbf{B}_d = \left(\mathbf{B} - \mathbf{B}_{obs}\right)$. L_f and L_d measure how well the force-free Eqs. (1) and divergence-free (2) conditions are fulfilled, respectively, and both $\omega_f(r,\theta,\phi)$ and $\omega_d(r,\theta,\phi)$ are weighting functions. For detailed description of the use of weighting functions, we direct the readers to Wiegelmann (2004). The term L_{photo} is surface integral over the photosphere which allows us to relax the field on the photosphere towards force-free solution without to much deviation from the original surface field data, $\mathbf{B}_{obs}$. In this integral, $\mathbf{W}(\theta,\phi)$ is a space-dependent diagonal matrix which gives different weights for observed surface field components depending on its relative accuracy in measurement.

The full inversion of SOLIS data is performed in the framework of Milne-Eddington model (ME)(Unno 1956). The inversion is made only for pixels whose polarization signal is above a selected threshold. Pixels with polarization below threshold are left undetermined. These data gaps represent a major difficulty for existing magnetic field extrapolation schemes. Therefore, those missing data is considered most inaccurate and are taken account of by setting $\mathbf{W}(\theta,\phi)$ to zero in all elements of the matrix. For the detailed description of the method we direct the readers to Wiegelmann and Inhester (2010) and Tadesse et al. (2011) for Cartesian and spherical geometry, respectively.

3 Results

In this study, we have used our spherical NLFFF optimization procedure to a group of active regions observed by SOLIS on October 11, 2011 and November 13, 2012. During the former observation, there were six active regions (ARs 11610, 11611, 11612, 11613, 11614 and 11615) and there were three vertically aligned active regions(ARs 11314, 11316, and 11319) in later one (see Fig. 1a and b). In order to accommodate the connectivity between those ARs and their surroundings, we adopt a non uniform spherical grid r, θ, and ϕ in the direction of radius, latitude, and longitude, respectively. Before applying our spherical NLFFF, we preprocessed the two photospheric vector field data sets using our spherical preprocessing routine.

There are no vector magnetic field measurements for the side and top boundaries of a localized domain. Therefore, we have to make assumptions about these fields before performing a NLFFF extrapolation. We assumed the lateral and upper boundaries of the computational domain as current-free. In order to initialize our NLFFF code, we calculated potential field from those data sets using their respective preprocessed radial field components ($\mathbf{B}_r$) using spherical harmonic expansion . The computational box is a wedge-shaped volume V with six boundary surfaces (four lateral side boundaries, top and photospheric boundaries). This box enables us to study the connectivities between active regions and their surroundings for the large field-of-views.

For computing the NLFFF field solutions for the two data sets, we use the preprocessed surface vector boundary fields with radial, longitudinal, and latitudinal components. We minimize the functional L_ω of Eq. (4). We implement the new term L_{photo} in Eq. (4) to treat those data gaps in SOLIS (Wiegelmann and Inhester 2010; Tadesse et al. 2011). For those pixels, for which $\mathbf{B}_{obs}$ was successfully inverted, we allow deviations between the model field $\mathbf{B}$ and the input fields observed $\mathbf{B}_{obs}$ surface field using Eq. (4), so that the model field can be iterated closer to a force-free solution even if the observations are inconsistent. We have used Langrangian multiplier of $\nu = 0.001$ to control the speed with which the lower boundary is injected during the NLFFF extrapolation.

In order to compare our reconstructions with observation, we plot the selected field lines of the NLFFF solutions for the two data sets and we overlay the field lines with corresponding AIA 193 Å image (see Figure 2c and d). From Figure 2c and d, one can see that the field lines of NLFFF model solutions are reconstructed in such away that they fit with the observation.

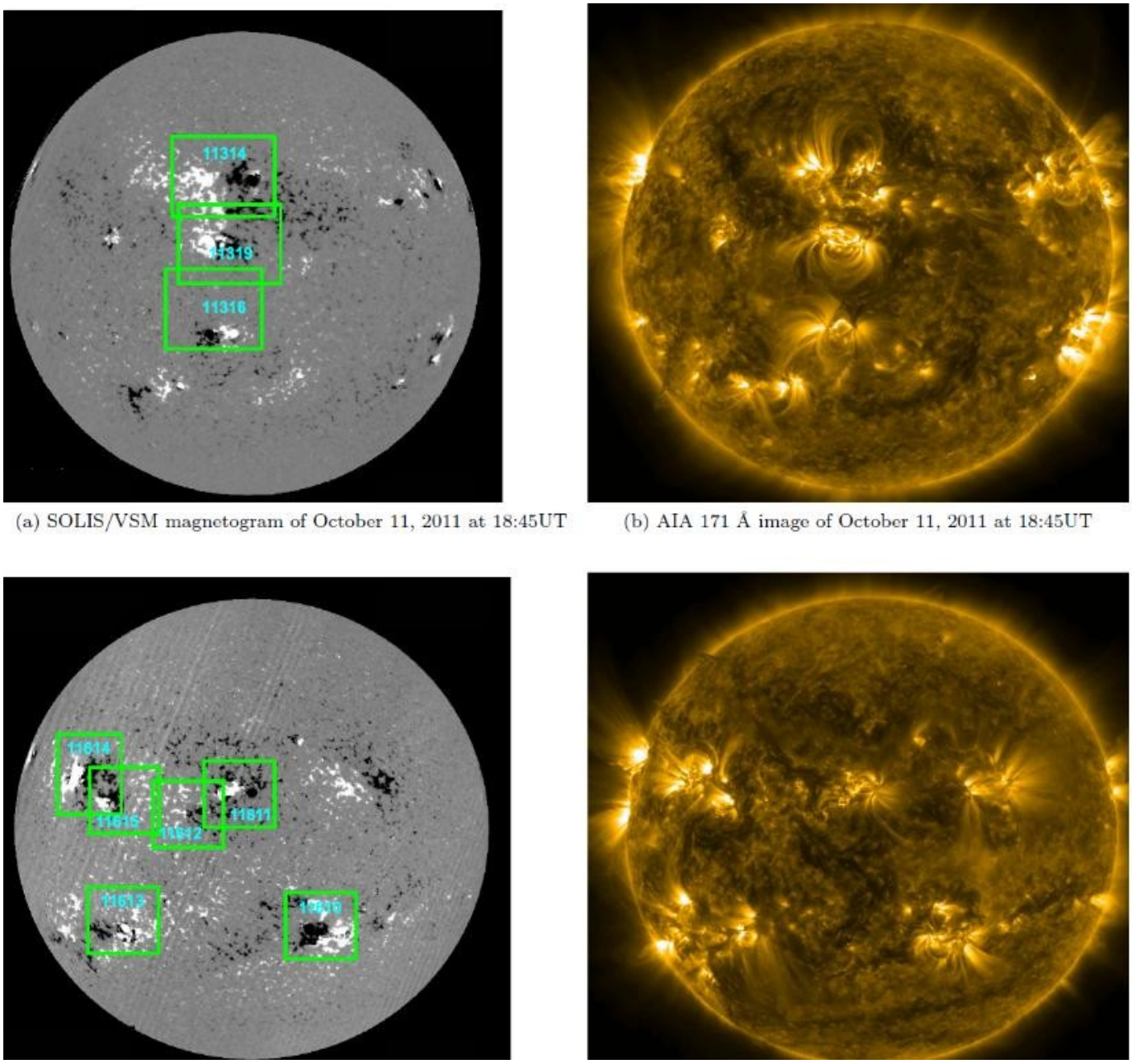

(a) SOLIS/VSM magnetogram of October 11, 2011 at 18:45UT

(b) AIA 171 Å image of October 11, 2011 at 18:45UT

Fig. 1 : a) Full-disk SOLIS/VSM magnetogram of October 11, 2011 at 18:45UT, b) Full-disk AIA 171 Å image of October 11, 2011 at 18:45UT, c) Full-disk SOLIS/VSM magnetogram of November 13, 2012 at 20:11UT, d) Full-disk AIA 171 Å image of of November 13, 2012 at 20:10UT. The blue boxes show the active regions observed.

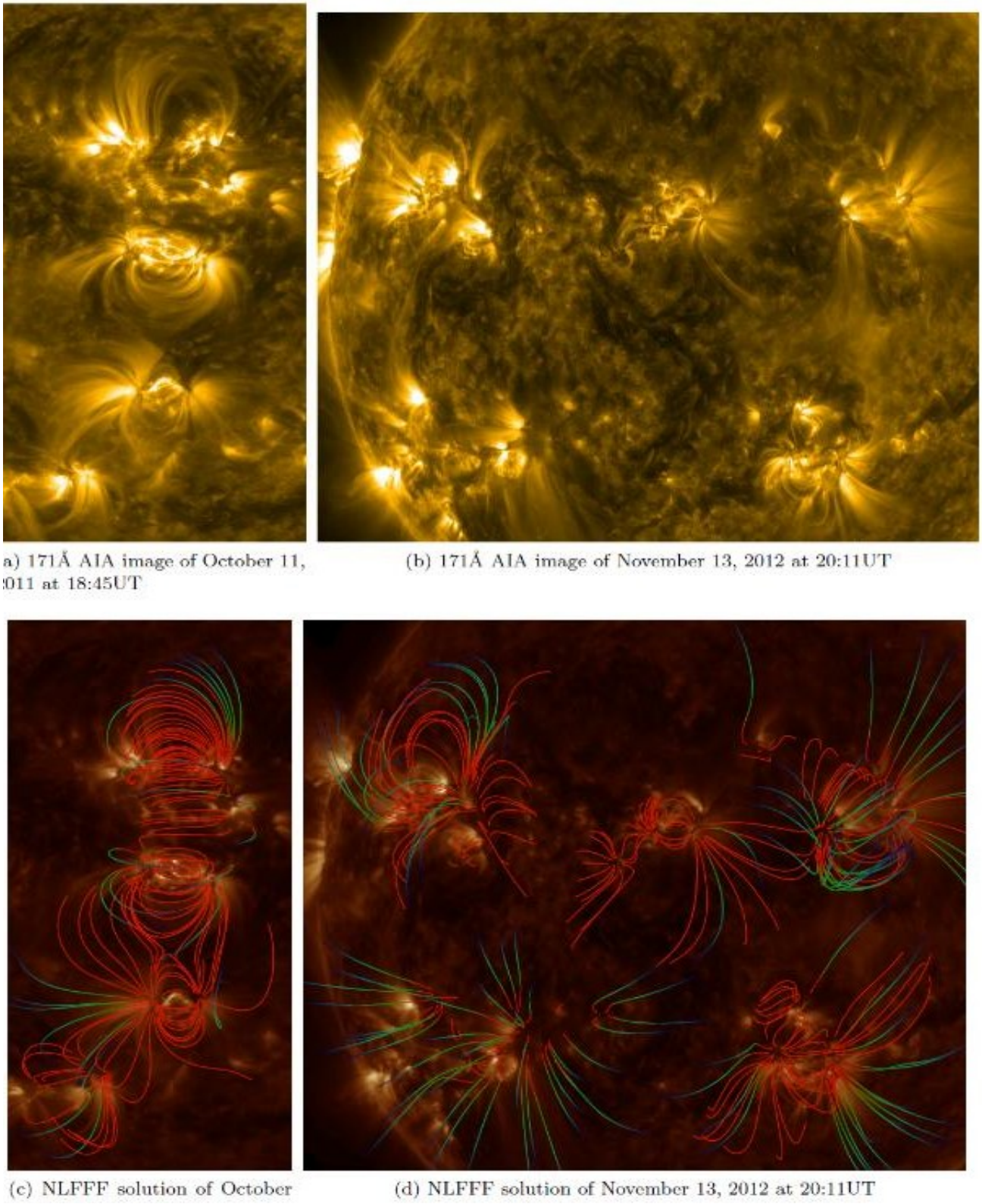

a) 171Å AIA image of October 11, 011 at 18:45UT

(b) 171Å AIA image of November 13, 2012 at 20:11UT

(c) NLFFF solution of October

(d) NLFFF solution of November 13, 2012 at 20:11UT

Fig. 2 : a) SDO/AIA 171 Å image on October 11, 2011 at 18:45UT, b) SDO/AIA 171 Å image on November 13, 2012 at 20:10UT, c) NLFFF model field lines of October 11, 2011 at 18:45UT overlaid on AIA 193Å image and d) NLFFF model field lines of November 13, 2012 at 20:11UT overlaid on AIA 193Å image. Green and red lines represent open and closed magnetic field lines.

There are spatial correspondence between the overall shape of the NLFFF field lines and the EUV loops for both observational dates. Those qualitative comparisons between NLFFF model magnetic field lines and the observed EUV loops of AIA images indicate that the NLFFF model provides a more consistent field for large field-of-views. Even if the qualitative nature is not ideal, it remains the best option in the absence of a more reliable quantitative comparison.

Once we have determined the 3D structure of the coronal magnetic field using the sophisticated numerical modeling, we can use those field solutions to calculate different quantities in the solar corona. We estimate the free magnetic energy to be the difference between the extrapolated NLFFF and the potential field with the same normal boundary conditions in the photosphereRégnier and Priest (2007); Thalmann et al. (2008). We therefore estimate the upper limit to the free magnetic energy associated with coronal currents of the form

$$E_{\rm free} = \frac{1}{8\pi}\int_V \left(B^2_{nlff} - B^2_{pot}\right) r^2 sin\theta dr d\theta d\phi, \qquad (5)$$

Our result for the estimation of free-magnetic energy in Table 1 shows that the NLFFF solutions have 2.13% and 6.28% more energy than the corresponding potential field solutions obtained from data observed on October 11, 2011 and November 13, 2012, respectively.

In our previous work Tadesse et al. (2012c), we have studied the connectivity between two active regions one in the northern hemisphere and the other in the south. In this study we have used the same method to calculate the percentage of the total electric current shared between the AR 11319 in the northern hemisphere and AR 11316 in the southern hemisphere observed on October 11, 2011 at 18:45UT (see Fig. 3). In order to quantify the percentage share in the electric current, we first identified those field lines carrying electric currents and emanating from AR 11319 and ending into AR 11316. The ratio of total electric current density flux due to those electric current carrying field lines connecting the two ARs to the total electric current density flux due to all field lines with current emanating from AR 11319 gives us the percentage share in the electric current between the two active regions. For this case study, we found that 23.31% of positive/negative polarity of AR 11319 in the northern hemisphere is connected to positive/negative polarity of AR 11316 in southern hemisphere. There are more electric current connectivity between these ARs as they are closer to each other even if they are located in different hemispheres. Therefore, during this particular observation, there are substantial number of trans-equatorial loops carrying electric current.

Table 1 : The magnetic energy associated with extrapolated 3D NLFFF field configurations from SOLIS data sets of the two dates.

Date	$E_{\rm total}(10^{33}{\rm erg})$	$E_{\rm free}(10^{33}{\rm erg})$
October 11, 2011	5.63	0.12
November 13, 2012	9.72	0.61

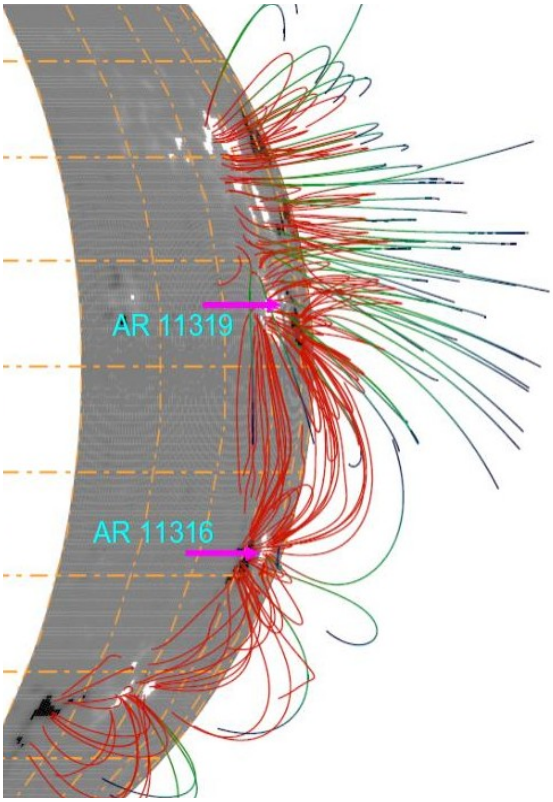

Fig. 3 : Selected field lines of NLFFF model solutions of October 11, 2011 at 18:45UT rotated to limb.

4 Conclusion and outlook

Coronal magnetic field modeling codes in Cartesian geometry are not well suited for larger domains, since the spherical nature of the solar surface cannot be neglected when the field of view is large. In this study, we have investigated the 3D coronal magnetic field associated with two data sets observed on October 11, 2011 and November 13, 2012 by analyzing SOLIS/VSM data using NLFFF model. During the former observation, there were six active regions (ARs 11610, 11611, 11612, 11613, 11614 and 11615) and there were three vertically aligned active regions in later one. We have used our

spherical NLFFF codes to compute the magnetic field solutions for large field of views with six active regions and three vertically aligned ones for the first time.

For the comparison with observations, we overlayed the NLFFF model field solutions for the two data sets with their respective EUV loops from AIA. The study indicates that there are significant agreements between EUV loops and NLFFF model solutions. There are spatial correspondence between the overall shape of the NLFFF field lines and the EUV loops for both observational dates. Those qualitative comparisons between NLFFF model magnetic field lines and the observed EUV loops of AIA images indicate that the NLFFF model provides a more consistent field for large field-of-views. Even if the qualitative nature is not ideal, it remains the best option in the absence of a more reliable quantitative comparison.

Today, Solar Dynamics Observatory (SDO) mission has been repeated observations of large, almost global scale events in which large scale connection between active regions may play fundamental role. Therefore, it is useful to implement a NLFFF procedure in spherical geometry for use when large scale boundary data are available, such as from the Helioseismic and Magnetic Imager (HMI) on board SDO. In order to handle large resolution data from HMI, one can adapt the multi-grid technique to the spherical code to improve its performance.

Acknowledgements SOLIS/VSM vector magnetograms are produced cooperatively by NSF/NSO and NASA/LWS. The National Solar Observatory (NSO) is operated by the Association of Universities for Research in Astronomy, Inc., under cooperative agreement with the National Science Foundation. This work was supported by NASA grant NNX07AU64G and the work of T. Wiegelmann was supported by DLR-grant 50 OC 453 0501.

References

DeRosa, M. L., Schrijver, C. J., Barnes, G. et al., 2009, Astrophys. J., 696, 1780

Gary G.A. 2001, Sol. Phys., 203,71

Guo, Y,, Ding, M.D., Liu, Y. et al., 2012, Astrophys. J.,760, 47

Jiang, C., Feng, X., 2012, Astrophys. J., 749, 135

Lin, H., Penn, M.J., Tomczyk, S., 2000, Astrophys. J. Lett., 541, 83

Liu, Y., Lin, H., 2008, Astrophys. J., 680, 1496

Malanushenko, A., Schrijver, C.J., DeRosa, M.L. et al., 2012, Astrophys. J., 756, 153

Régnier, S., Priest, E.R., 2007, Astrophys. J. Lett., 669, 53

Schrijver, C.J., Title, A.M., 2005, Astrophys. J., 619, 1077

Tadesse, T., Wiegelmann, T., Inhester, B., 2009, Astron. Astrophys., 508, 421

Tadesse, T., Wiegelmann, T., Inhester, B. et al., 2011, Astron. Astrophys., 527, 30

Tadesse, T., Wiegelmann, T., Inhester, B. et al., 2012, Sol. Phys., 281, 53

Tadesse, T., Wiegelmann, T., Inhester, B. et al., 2012, Sol. Phys., 277, 119

Tadesse, T., Wiegelmann, T., Inhester, B. et al., 2012, ArXiv e-prints

Tadesse, T., Wiegelmann, T., Inhester, B. et al., 2012, Astron. Astrophys., 550, 14

Thalmann, J.K., Wiegelmann, T., Raouafi, N.-E., 2008, Astron. Astrophys., 488, 71

Unno, W., 1956, Publ. Astron. Soc. Japan, 8, 108

Wheatland, M.S., Leka, K.D., 2011, Astrophys. J., 728, 112

Wheatland, M.S., Régnier, S., 2009, Astrophys. J. Lett., 700, 88

Wheatland, M.S., Sturrock, P.A., Roumeliotis, G., 2000, Astrophys. J., 540, 1150

Wiegelmann, T., 2004, Sol. Phys., 219, 87

Wiegelmann, T., Sol. Phys., 240, 227

Wiegelmann, T., Inhester, B., 2010, Astron. Astrophys., 516, 107

Wiegelmann, T., Sakurai, T., 2012, Living Reviews in Sol. Phys., 9, 5

Wiegelmann, T., Inhester, B., Sakurai, T., 2006, Sol. Phys., 233, 215

Wiegelmann, T., Thalmann, J. K., Inhester, B. et al., 2012, Sol. Phys., 281, 37